ISBN: 978-3-95450-241-7 ISSN: 2673-5350 doi:10.18429/JACoW-IBIC2022-TUP20

CORRECTIONS FOR SYSTEMATIC ERRORS IN TRANSVERSE PHASE SPACE MEASUREMENTS AT PITZ

C. Richard*, Z. Aboulbanine, G. Adhikari, N. Aftab, P. Boonpornprasert, G. Georgiev, M. Gross, A. Hoffmann, M. Krasilnikov, X.-K. Li, A. Lueangaramwong, R. Niemczyk, H. Qian, F. Stephan, G. Vashchenko, T. Weilbach, Deutsches Elektronen-Synchrotron DESY, Zeuthen, Germany

Abstract

The Photo Injector Test Facility at DESY in Zeuthen (PITZ) characterizes and optimizes electron sources for use at FLASH and European XFEL. At PITZ, the transverse phase space is measured using a single slit scan and scintillator screen method. With the trend in photoinjectors towards lower current and emittance, these measurements become increasingly influenced by systematic errors including camera resolution and scintillator response due to smaller spot sizes. This study investigates the effects and corrections of the systematic errors for phase space measurements at PITZ.

INTRODUCTION

The Photo Injector Test Facility at DESY in Zeuthen (PITZ) commissions and characterizes electron guns for use in Free Electron Lasers (FEL) at FLASH and European XFEL [1]. For FEL operation, the transverse emittance is a key parameter for optimizing the gain length [2]. To characterize the electron guns, PITZ measures the emittance using a single slit emittance scanners. These devices measure the transverse phase space by stepping a narrow slit through the beam to only allow particles at a given position to pass. The profiles of passed beamlets are measured with a camera capturing the signal on a downstream scintillator screen to measure the angular distribution [3]. The systematic errors in this system have previously been studied for the PITZ emittance scanners [4, 5] and it was found that one of the primary systematic errors in this system is the resolution of the camera. However, these studies focused on the effect of the camera resolution on full beam measurements not beamlet measurements and do not quantify the effects on the measured emittance. The effect of the slit width on the measured emittance has also be been estimated [6, 7], but, for simplification, it was assumed the beam had no $x - x'$ coupling and the camera effects were excluded. In addition, previous studies do not propose corrections for the systematic errors and it is desired to correct for these errors so accurate emittance measurements can be made.

SYSTEMATIC ERRORS FROM SLIT SIZE

To measure the transverse position profile, the emittance scanner uses a 50 µm slit that is stepped across the beam. With this method, the measured profile is the convolution of the beam profile with the slit opening. Therefore, the measured rms beam size $\sigma_{x,m}$ can be corrected using

$$\sigma_{x,m}^2 = \sigma_{x,t}^2 + \sigma_s^2 \ , \qquad (1)$$

* christopher.richard@desy.de

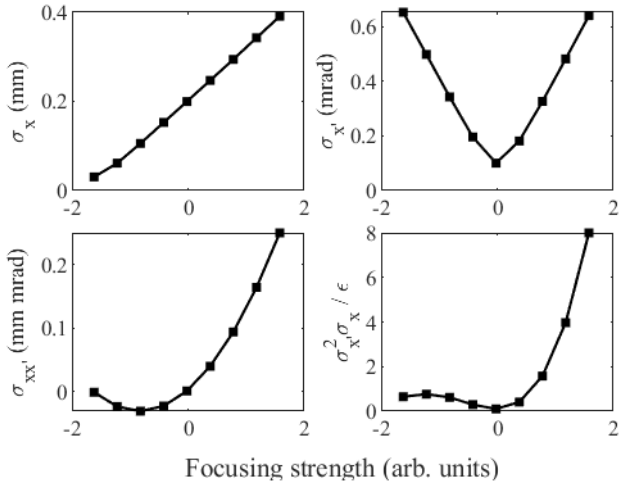

Figure 1: rms parameters of the synthetic optics scan used to test the correction methods. The geometric emittance is 0.02 mm·mrad.

where $\sigma_{x,t}$ is the true rms beam size and $\sigma_s = 50\,\mu\text{m}/\sqrt{12} \approx 14\,\mu\text{m}$ is the rms size of the slit. This results in a ~0.5% increase in $\sigma_{x,m}$ when $\sigma_{x,t} \approx 0.15$ mm which is typical at PITZ and ~5% error when $\sigma_{x,t} \approx 0.05$ mm. This also effects the measured geometric emittance measured rms emittance

$$\epsilon_m = \sqrt{\sigma_{x,m}^2 \sigma_{x',m}^2 - \sigma_{xx',m}^2} \ , \qquad (2)$$

where $\sigma_{x,m}^2 =< x^2 >$, $\sigma_{x',m}^2 =< x'^2 >$, and $\sigma_{xx',m} =< xx' >$ is a correlation term. The measured emittance can be corrected by the substitution $\sigma_{x,m}^2 \rightarrow \sigma_{x,m}^2 - \sigma_s^2$ into Eq. (2).

To study the effect on the measured emittance, a linear model of the emittance scanner was made in Matlab [8]. The model takes particles from an 4D input distribution and separates them into beamlets based on their x position replicate the slit mask. Each beamlet is then propagated through a drift length to the screen location and heat maps of the particle densities are made to replicate the screen response. To simulate beams with a range parameters similar to what is measured at PITZ, a Gaussian distribution is generated with geometric emittance $\epsilon_g = 0.02$ mm·mrad, put through a thin lens kick and a 30 cm drift length, then processed with the emittance scanner model. The resulting beam parameters at the start of the emittance scanner are shown in Fig. 1.

The measured, uncorrected rms emittance increases as the beam size decreases as expected from Eq. (1) and can be corrected (see Fig. 2). However, the emittance also significantly

ISBN: 978-3-95450-241-7 ISSN: 2673-5350 doi:10.18429/JACoW-IBIC2022-TUP20

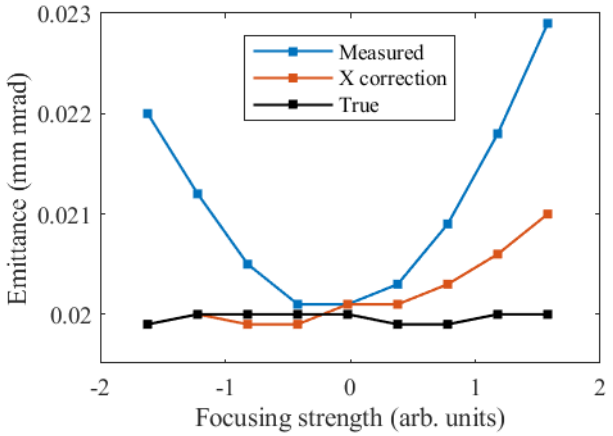

Figure 2: The rms geometric emittance increases due to the slit size as the beam size decreases. It also increases at large beam sizes due to the large $x - x'$ coupling causing the emittance to be very sensitive to the calculated rms values. Variation in the true emittance are due to statistical fluctuations.

increases when the beam size is large. This is caused by the strong $x - x'$ coupling making the calculated emittance sensitive to small changes in any of the rms parameters. The sensitivity of the emittance is found by taking the derivative with respect to σ_x

$$\mathrm{d}\epsilon = \frac{\sigma_{x'}^2 \sigma_x}{\epsilon} \mathrm{d}\sigma_x. \tag{3}$$

Due to this sensitivity, using Eq. (1) to correct the emittance improves the measured value, but does not completely correct for the effect of the slit. To avoid this sensitivity to small changes in the rms parameters, measurements should be taken when $\sigma_{x'}^2 \sigma_x / \epsilon \lesssim 1$.

CAMERA RESOLUTION SYSTEMATIC ERRORS

The non-zero pixel size of the camera causes the camera to have a point spread function (PSF), i.e. the camera will record a finite sized signal form an infinitesimally sized input signal. This causes the images recorded by the camera to be a convolution of the true image with the PSF. This can cause a significant increase in the measured size of the beamlets size when the true rms size is comparable to the rms size of the PSF.

Determining the Point Spread Function

Assume the PSF is Gaussian with standard deviation σ_p

$$p(x) = \frac{1}{\sqrt{2\pi}\sigma_p} e^{-\frac{x^2}{2\sigma_p^2}}. \tag{4}$$

The rms size of the PSF is related to camera's optical resolution with the modulation transfer function z (MTF) [5]

$$z(\omega) = \int_{-\infty}^{\infty} p(x) e^{-i\omega x} dx = e^{-\frac{1}{2}\sigma_p^2 \omega^2}. \tag{5}$$

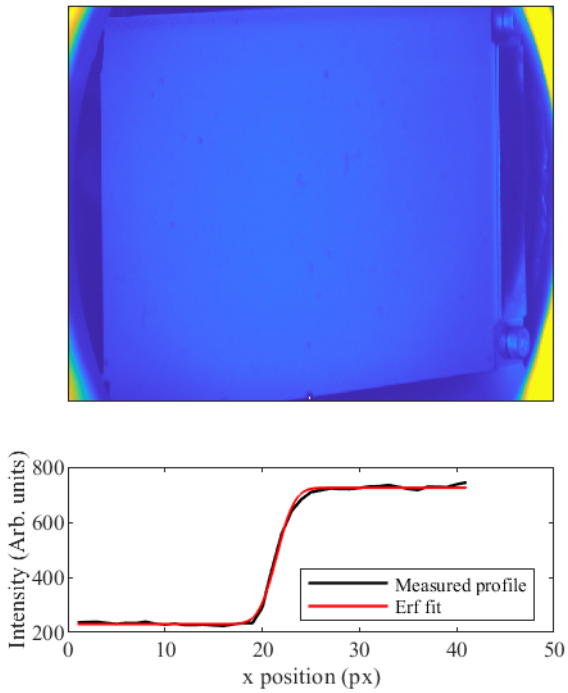

Figure 3: Image of an scintillator screen with a light shining on it (top). The intensity profile of the left edge of the screen was fitted to an error function to determine the rms PSF (bottom).

The optical resolution ω_0 in px/mm of the camera can be defined by

$$z(\omega_0) = 0.1 \tag{6}$$

which gives

$$\sigma_p = \sqrt{2\ln(10)} \approx 2.14 \text{ px}. \tag{7}$$

This can be converted to a length by dividing by ω_0. For the presented measurements, the camera's optical resolution is $\omega_0 = 28.8$ px/mm giving an rms PSF $\sigma = 74$ µm.

The rms size of the PSF can be verified by using an image taken at a screen station with a light illuminating the screen. On the edges of the image, metal brackets can be seen that hold the scintillator screen (see Fig. 3). Assuming the brackets have a hard edge and the PSF is Gaussian, then the intensity profile across the edge will be an error function corresponding to the integral of the PSF. For the image in Fig. 3, the intensity profile of 50 rows of pixels at the center of the left edge were fit to an error function. The measured rms PSF was $\sigma_p = 2.01 \pm 0.11$ px which agrees the theoretical MTF approach.

PSF Effects on Measured Distributions

The camera in the emittance scanner measures the response of the scintillator screen from beamlets that pass through the slit. The angular profile of the beam at the slit

ISBN: 978-3-95450-241-7 ISSN: 2673-5350 doi:10.18429/JACoW-IBIC2022-TUP20

location is assumed to be proportional to the spatial profile of the passed beamlet. However, the recorded images are the 2D convolution of the true screen responses with the PSF. Therefore, the measured rms beamlet sizes σ_{bl_m} can be estimated as

$$\sigma_{bl,m}^2 = \sigma_{bl,t}^2 + \sigma_p^2 \ , \tag{8}$$

where σ_{bl_t} is the true rms beamlet size. Assuming a the size of the slit is negligible, the rms size of the beamlet on the screen can be related to the rms parameters of the beam

$$\sigma_{bl,t} = \frac{\epsilon_t}{\sigma_{x,t}} L = L\sqrt{\sigma_{x',t}^2 - \frac{\sigma_{xx',t}^2}{\sigma_{x,t}^2}} \ , \tag{9}$$

where $L = 3.133$ m is the drift length between the slit and the screen. Assuming $\sigma_{xx',t} \approx 0$ and $\sigma_{x',t} \approx 0.15$ mrad then $\sigma_{bl,t} \approx 0.3$ mm. Using Eq. (8) and $\sigma_p = 74$ µm, this results in a ~3% increase in the measured beamlet size.

To study the effect of the PSF, the Matlab model of the emittance scanner was modified to convolved the heat maps of the beamlet particle densities with a Gaussian PSF with σ_p defined by Eq. (7). In addition, Gaussian noise can be added then removed from the images to replicate the image processing.

When the beamlet distributions are convolved with the PSF, the increase in the measured emittance is dominated by the effect of the slit size for small σ_x (i.e. lower focusing strength in Fig. 4 top). As the focusing strength and $\sigma_{x,t}$ increase, firstly, $\sigma_{x'}$ becomes small causing the beamlet sizes to decrease, resulting in a larger increase on their measured size due to the PSF, and therefore a larger measured emittance. As the focusing strength continues to increase, all $\sigma_{x',t}$ and $\sigma_{xx',t}$ start to increase (see Fig. 1). This increases the sensitivity of the measured emittance to the measured rms value and the error continues to increase. In these regions, there is ~5% increase in the measured emittance compared to the case without convolving with the PSF.

The effects of the slit and PSF can result in >20% increase in the measured emittance if $\sigma_{x,t}$ or $\sigma_{x',t}$ is too small or $\sigma_{xx',t}$ is too large. These effects are significant enough that even when Gaussian noise was added at 1% of the peak intensity then removed, the measured emittance can still be larger than the 100% emittance (see Fig. 4). The noise 1% noise level is a rough upper bound to measurements taken at PITZ with typical noise levels being around 0.5%.

Beamlet Image Correction

In order to correct for the effects of the camera resolution, the beamlet images must be deconvolved from the PSF. The best results for the 2D deconvolution were achieved using 5 iteration of the Richardson-Lucy algorithm with a regularization parameters of 0.1 [9]. In addition, the effect of the slit size is corrected as described above. Note, the corrected emittances should be compared to the true emittances but rather the emittances from images without the PSF convolution and with the slit correction applied $\epsilon_{\text{slit},c}$ as these are

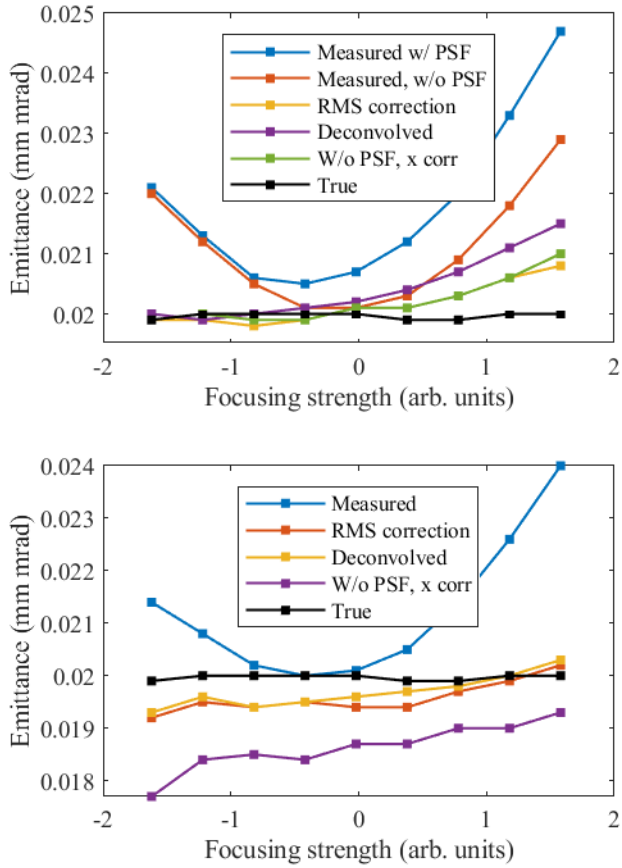

Figure 4: Measured and corrected rms geometric emittances for the cases with no noise present (top) and noise added then removed (bottom). The corrected values should be compared to the case of "W/o PSF, x corr", i.e. no PSF effects and corrected with Eq. (1), rather than the true emittance as this is the measured result without convolving with the PSF.

the best achievable results. Without added noise, deconvolving the beamlet images corrects for effects of the PSF on the emittance to <3% of $\epsilon_{\text{slit},c}$ for the simulated parameter range (see Fig. 4). The deconvolution does not reproduce the exact emittance because deconvolution algorithm was optimized assuming the presence of noise which causes the deconvolution process to be noisy and ill-posed problem. Therefore, when tuning the algorithm, the suppression of artifacts was valued more than exact replication.

While the deconvolution algorithm improves the measured emittance, it is slow, taking upward of 2.5 min depending on the number of beamlet images, and can possibly lead to nonsensical results due to noise. Instead, if detailed phase space measurements are not required, it may preferable to only correct the rms parameters. By plugging Eq. (9) into Eq. (8) and assuming the measured beamlet size also follows Eq. (9) but using the measured rms parameters, the correction to $\sigma_{x',m}$ can be approximated by

$$\sigma_{x',m}^2 = \sigma_{x',t}^2 + \sigma_p^2/L^2 \ , \tag{10}$$

where $\sigma_{x',m}$ is the measured rms angle and $\sigma_{x',t}$ is the true rms angle. This effectively assumes the x' distribution was

ISBN: 978-3-95450-241-7 ISSN: 2673-5350 doi:10.18429/JACoW-IBIC2022-TUP20

convolved with a Gaussian with rms size σ_p/L instead of the individual beamlets being convolved. Applying this correction to the measured emittance results in agreement within 1% to $\epsilon_{\mathrm{slit},c}$.

In the case when noise is added then removed (see Fig. 4 bottom), the two PSF correction methods agree with each other within 2%. However, the agreement with the non-convolved, slit corrected results is spoiled across the entire beam parameter range. This may be caused by the convolved beamlets being larger than the non-convolved ones and therefore, the noise cut had less of an effect on the measured beamlet sizes.

MEASURED RESULTS

These corrections for the PSF can be applied to measurements taken at PITZ. The results in Fig. 5 are from a typical scan of the strength of a solenoid magnet located at the electron gun to find the current setting with minimum emittance for a 19.5 MeV, 250 pC beam. When the PSF and slit corrections are applied the measured emittance is reduced by 3 - 15% and the results from the 2D deconvolution and the rms parameter correction agree within 2% (see Fig. 5). For these measurements, $\sigma_x'^2\sigma_x/\epsilon < 1$ therefore the errors due to large $\sigma^2_{xx'}$ are minimal. The measured rms sizes are $\sigma_x \approx 0.2$ mm and $\sigma_{x'} \approx 0.15$ mrad. Using Eqs. (1) and (10), the corrections for the slit size will be <0.5% and corrections for the PSF will be ~3% which roughly agrees with the measured values for lower solenoid currents. These corrections shift the minimum measured emittance setting of the solenoid by 1 A which can have an impact on the beam dynamics and tuning of the accelerator.

CONCLUSION

Phase space measurements at PITZ using a single slit scanner can be improved by correcting the beamlet images for the effects of the camera PSF and slit size. The correction can be performed by deconvolving the measured beamlet images or by applying corrections to the measured rms parameters. The measured emittance is significantly affected when the beam size is comparable to the slit size and when the beamlet size at the scintillator screen is comparable to the rms PSF. Both of these cases can be reliably corrected. However, when the beam is strongly $x - x'$ coupled, the measured emittance becomes very sensitive to the exact measured size and the measurements become unreliable.

These corrections improve the dominant linear systematic errors and help define a range of beam parameters where the emittance measurements can be trusted. However, in addition, future studies must be conducted to correct for non-linear effects such as space charge effects on the beamlets [4] and the non-linear response of the scintillator [10].

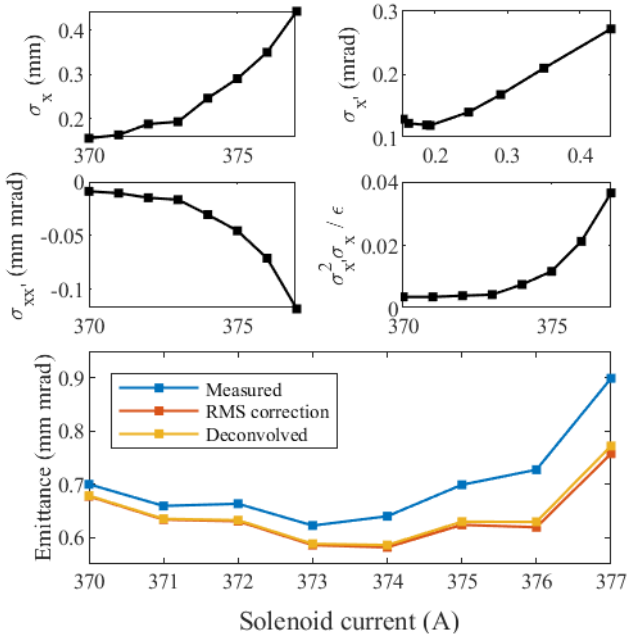

Figure 5: Measured rms parameters of the at the emittance scanner for a range of gun solenoid currents. The corrections reduce the measured emittance by 3 - 15% can change the solenoid current for the minimum emittance from 373 A to 374 A.

REFERENCES

[1] M. Krasilnikov *et al.*, "Experimentally minimized beam emittance from an *L*-band photoinjector", *Phys. Rev. ST Accel. Beams*, vol. 15, p. 100701, 2012. doi:10.1103/PhysRevSTAB.15.100701

[2] E. J. Jaeschke *et al.*, *Synchrotron Light Sources and Free Electron Lasers*, p. 155, Springer International Publishing, Switzerland, 2016. doi:10.1007/978-3-319-14394-1

[3] L. Staykov, "Design Optimization of an Emittance Measurement System at PITZ", in *Proc. DIPAC'05*, Lyon, France, Jun. 2005, paper POT032, pp. 220–222.

[4] L. Staykov, "Characterization of the transverse phase space at the photo-injector test facility in DESY, Zeuthen site", Ph.D. thesis, University Hamburg, Hamburg, Germany, 2008.

[5] R. Spesyvtsev, "Transverse Beam Size Measurement Systems at Photo Injector Test Facility in Zeuthen", master's thesis, Karazin Kharkiv National University, Kharkiv, Ukraine, 2007.

[6] R. Niemczyk, "Subpicosecond-resolved emittance measurements of high-brightness electron beams with space charge effects at PITZ", Ph.D. thesis, University Hamburg, Hamburg, Germany, 2021.

[7] G. Vashchenko, "Tranverse Phase Space Studies with the New CDS Booster Cavity at PITZ", Ph.D. thesis, University Hamburg, Hamburg, Germany, 2013.

[8] The MathWorks Inc., MATLAB, version 9.9.0.1570001 (R2020b), Natick, Massachusetts, 2020.

[9] D. Biggs and M. Andrews, "Acceleration of Iterative Image Restoration Algorithms", *Appl. Opt.*, vol. 36, no. 8, pp. 1766-1775, 1997. doi:10.1364/AO.36.001766

[10] G. Kube, S. Liu, A. I. Novokshonov, and M. Scholz, "A Simple Model to Describe Smoke Ring Shaped Beam Profile Measurements With Scintillating Screens at the European XFEL", in *Proc. IBIC'18*, Shanghai, China, Sep. 2018, pp. 366–370. doi:10.18429/JACoW-IBIC2018-WEOC03